A Technique for Detecting a Tropical Cyclone Center Using a Doppler Radar

VINCENT T. WOOD

NOAA, Environmental Research Laboratories, National Severe Storms Laboratory, Norman, Oklahoma

(Manuscript received 30 June 1993, in final form 7 January 1994)

ABSTRACT

A ground-based Doppler radar technique is developed for detecting a tropical cyclone center position. Accurate determination of the cyclone center position, based on Doppler velocity measurements, will become essential for the issuance of hurricane advisories, forecasts, and warnings once a network of WSR-88D Doppler radars is deployed on the United States coastlines, islands, and military bases during the 1990s. This will allow high-resolution detection and tracking of hurricanes nearing land for the first time.

Simulated Doppler velocity data, which were reconstructed from wind field data collected by reconnaissance aircraft during Hurricanes Alicia (1983) and Gloria (1985), were used to test the concept of using ground-based Doppler radar data to estimate cyclone center location. The center range and azimuth estimates of a hurricane signature were calculated from the simulated coastal Doppler radar velocity data. Preliminary results indicate that the technique performed well for estimating center locations from the radar measurements compared with storm center positions determined from in situ aircraft measurements.

1. Introduction

Radar has been a valuable tool in tracking tropical cyclones since the first radar observations of tropical cyclones began in the late 1940s (Maynard 1945; Wexler 1947). Major radar networks were established in Japan and the United States in the late 1950s primarily to track tropical cyclones. With the deployment of the Weather Surveillance Radar-1988 Doppler (WSR-88D) system during the 1990s, the potential for routinely tracking tropical cyclones nearing land can be realized. Because of their Doppler velocity-measuring capabilities, these S-band (10-cm wavelength) radars have the potential to increase the accuracy and timeliness of hurricane advisories, forecasts, and warnings (Baynton 1979; Jorgensen 1982; Zipser et al. 1990) through improved observations of a storm center's track and intensity.

Many techniques were devised to identify and track tropical cyclones using noncoherent radars, weather satellites, and hurricane reconnaissance missions. Senn et al. (1957) and Senn and Hiser (1959) developed a technique that utilized a logarithmic spiral fit to the rainband positions to estimate a tropical cyclone center. Sivaramakrishnan and Selvam (1966) devised a spiral overlay technique used in conjunction with cloud photographs obtained by a weather satellite to locate a hurricane's center. Willoughby and Chelmow (1982) developed an objective procedure to estimate the dynamic center of a hurricane based on the flight-level wind and D value (the departure of a selected isobaric height from its value in the standard atmosphere).

Timely and accurate estimates of the center position and motion of a tropical cyclone by the WSR-88D radar are essential for hurricane surveillance when reconnaissance aircraft and satellite estimates are unavailable or available too infrequently to provide the desired degree of time and space continuity. Furthermore, they are among the more important parameters to be determined from the WSR-88D radars because they are needed as input not only to the hurricane forecasters but to tropical cyclone algorithms as well. For example, the tropical cyclone center position was used by Donaldson (1991), Lee et al. (1993), and Roux (1993) for diagnosis of hurricane structure.

This paper describes a computer technique that detects a tropical cyclone center position based on Doppler velocity measurements. Section 2 discusses an analytical flow model that is used to simulate a single-Doppler velocity field corresponding to an idealized tropical cyclone. Section 3 describes the concept of a pattern recognition technique that is a useful tool for single-Doppler radar identification of atmospheric vortices such as a tropical cyclone or a thunderstorm mesocyclone circulation. The computer technique incorporates azimuthal shear and velocity difference thresholds for detecting tropical cyclones and making estimates of the center location from the radar measurements. In section 4, the technique is evaluated to determine its ability to detect a tropical cyclone. Simulated single-Doppler velocities are reconstructed from the wind fields for Hurricanes Alicia (1983) and Gloria (1985), and the hurricane center positions estimated from the radar are compared with in situ aircraft mea-

Corresponding author address: Vincent T. Wood, NOAA/ERL/NSSL, 1313 Halley Circle, Norman, OK 73069.

surements. Conclusions and future research problems are discussed in section 5.

2. The analytical flow model

A simple analytical model (e.g., Brown and Wood 1991; Wood and Brown 1992) can be used to approximate the basic horizontal flow field within a tropical cyclone vortex; the model specifies, to a first approximation, axisymmetric velocity distributions (Hughes 1952; Riehl 1954, 1963; Gray and Shea 1973). According to the distributions, tangential velocity increases linearly from a circulation center where velocity is zero to a core radius where the tangential velocity attains its maximum value. Beyond the core radius, the tangential velocity decreases in a manner inversely proportional to distance from the circulation center. Mathematically, the velocity distribution for the tangential, $v_t(r)$, wind component in the Rankine (1901) combined vortex flow model is given by

$$v_t(r) = V_t\left(\frac{r_c}{r}\right)^{\lambda}, \qquad (1)$$

where V_t is the peak tangential velocity at the core radius r_c, and r is the distance from the circulation center. The exponent λ describes the radial profile of the tangential wind component. Inside the radius of maximum wind (RMW), $\lambda = -1$ is often assumed. Outside the RMW, λ generally lies between 0.4 and 0.6 (Hughes 1952; Riehl 1954, 1963; Gray and Shea 1973).

The Doppler velocity component V_d at slant range R is the component of the wind vector in the viewing direction θ, from a radar. As derived by Wood and Brown (1992), the Doppler velocity value at R, θ is given by

$$V_d = \frac{2V_t}{\alpha}\left(\frac{r_c}{r}\right)^{\lambda+1}\sin(\theta - \theta_c), \qquad (2)$$

where $r = [R_c^2 + R^2 - 2R_cR\cos(\theta - \theta_c)]^{1/2}$ is the radial distance from the circulation center; R_c, θ_c represents the center range and azimuth, respectively, of the modeled flow feature from the radar; and a dimensionless aspect ratio α is defined as the ratio of core diameter $2r_c$ to range R_c of a circulation center from the radar. The procedure for generating a simulated Doppler velocity field in (2) was outlined by Wood and Brown (1992). The velocity field contains some additional simplifying assumptions. The vertical component of motion is not simulated; therefore, the radar measurements are assumed to be made at low elevation angles. Furthermore, the simulation assumes that the radar measurements are free of noise and that the radar beam has an infinitesimal width (producing perfect radar resolution at all ranges, rather than degraded resolution at far ranges).

Figure 1 depicts a horizontal scan through a modeled hurricane vortex rotating cyclonically around a vertical axis, and the associated single-Doppler velocity pattern

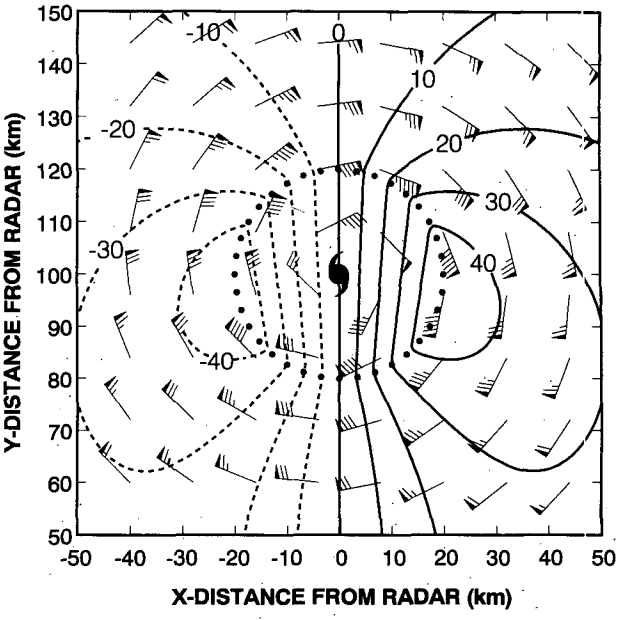

FIG. 1. Plan view of an axisymmetric hurricane vortex flow (wind vectors) and the corresponding single-Doppler velocity signature for a radar located 100 km south of the vortex center. The wind plotting convention is flag, 25 m s^{-1}; barb, 5 m s^{-1}; and half-barb, 2.5 m s^{-1}. Doppler velocities are contoured. Solid curves represent flow away from the radar (positive Doppler velocities), with the exception that the zero Doppler velocity contour is the first solid contour; dashed curves represent flow toward the radar (negative Doppler velocities). The contour interval is 10 m s^{-1}. The hurricane center is indicated by the hurricane symbol. The dotted circle surrounding the hurricane center is the location of maximum wind speed.

that would be measured by a Doppler radar due south of the vortex center (R_c = 100 km, $\theta_c = 0°$, α = 0.4, in this case). The radial velocity structure of a hurricane at low elevation angle is similar to that of a thunderstorm mesocyclone detected by a single Doppler radar (Burgess and Ray 1986; Brown and Wood 1983, 1991; Burgess and Lemon 1990), except that the hurricane is roughly ten times larger in diameter.

3. Pattern recognition technique

The pattern recognition technique used here relies on identification of the main attribute that an atmospheric phenomenon (e.g., thunderstorm mesocyclone or tropical cyclone circulation) produces in the Doppler velocity field. The pattern recognition technique was used, for example, by Zrnić et al. (1985) and Desrochers and Donaldson (1992) to search successive radar-viewing azimuths for increases of Doppler velocities in order to detect thunderstorm mesocyclones. In the technique, when a run of increasing velocities ends, the beginning and ending velocity data points of the run define a shear segment, represented by curved arrows in Fig. 2. The main attributes of the shear segment, which are consolidated into a seven-component pattern vector, consist of the slant range (R), the beginning and ending azimuth angles (θ_b, θ_e), the beginning and

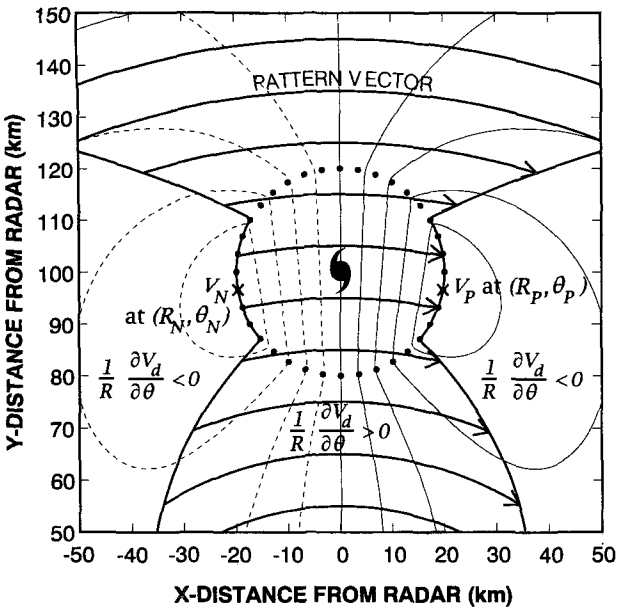

FIG. 2. Single-Doppler velocity pattern of the hurricane vortex (heavy solid curves representing the region of positive azimuthal Doppler shear). A curved arrow represents a shear segment. The Doppler velocity contour convention and the hurricane center are as in Fig. 1. Here, V_N and V_P represent extreme negative and positive Doppler velocity values located at range and azimuthal points (R_N, θ_N) and (R_P, θ_P), respectively, as indicated by crosses.

ending Doppler velocity values (V_b, V_e), and the beginning and ending times (t_b, t_e) at both ends of the shear segment. Here, beginning b and ending e subscripts refer to a clockwise radar sweep. When pattern vectors are consolidated into a two-dimensional shear feature, pattern vectors jointly provide information on the circulation size, strength, and rotational velocity.

For identifying the tropical cyclone vortex, the most important parameter is the sign of the azimuthal velocity gradient. Azimuthal shear is defined here as the shear of Doppler velocities in the azimuthal direction, and for a pattern vector, it is given by

$$S = \frac{\Delta V}{R(\theta_e - \theta_b)}, \tag{3}$$

where $\Delta V = V_e - V_b$ is the velocity difference and $R(\theta_e - \theta_b)$ represents the azimuthal distance across the shear segment. In Fig. 2, heavy solid curves to the left and right of the hurricane center represent the lines along which Doppler velocity peaks occur. They are, respectively, bounded by data points (R_b, θ_b) and (R_e, θ_e). The azimuthal Doppler shear changes sign at these points, thus satisfying $\partial V_d/\partial\theta = 0$. The shear of the pattern vector region is characteristic of tropical cyclones and is useful for tropical cyclone identification.

a. Tropical cyclone detection

The detection of a tropical cyclone vortex commences by searching for cyclonic shear (i.e., $S > 0$) across adjacent radials of Doppler velocity data. This is accomplished by identifying increasing velocities at constant range in the clockwise azimuthal direction. If positive shear exists, a pattern vector is "opened." The procedure continues for the next two radials, and so on until positive shear is no longer detected for that range and the pattern vector is "closed." Two parameters, velocity difference ΔV and azimuthal shear S, are then calculated, and if these quantities exceed predetermined detection thresholds, the seven-component pattern vector is saved for further analysis, as indicated by the curved arrows in Fig. 3a. In this example, the velocity difference and azimuthal shear detection thresholds are 50 m s^{-1} and 1 m s^{-1} km^{-1}, respectively.

At the end of an elevation scan, individual pattern vectors that are oriented perpendicular to the radar beam are then grouped together into a two-dimensional shear feature according to their spatial proximities. The vectors whose azimuthal extents overlap, and that are separated in range by no more than 1 km, are combined into a common feature. If the total number of vectors in a completed feature is less than a preset threshold, the feature is discarded.

The next step is to determine the locations of extreme Doppler velocity values, where the maximum tangential flow at the RMW of a hurricane vortex is measured. As depicted in Fig. 2, the maximum velocities of the vortex core can easily be observed by the Doppler radar only at the two points where tangential velocity is directed along the radar beam. As shown in the figure, the range and azimuth of the extreme negative Doppler velocity value V_N on the left side of the vortex signature center, as viewed from the Doppler radar, are represented by (R_N, θ_N); the range and azimuth of the extreme positive velocity value V_P on the right side are represented by (R_P, θ_P).

The technique of Desrochers and Donaldson (1992) was followed for isolating the velocity maxima of a couplet. They searched for the beginning and ending velocities for every pattern vector of a feature for the positive and negative velocity extrema. The pattern vector is included in the sample if its magnitude is within some velocity difference threshold ΔW of the maximum velocity of all the kth pattern vectors. The velocity, range, and azimuth on each side of the velocity couplet are computed as weighted averages,

$$\left.\begin{aligned} V_N &= \frac{\sum_k (V_b)_k W}{\sum_k W} \\ R_N &= \frac{\sum_k (R)_k W}{\sum_k W} \\ \theta_N &= \frac{\sum_k (\theta_b)_k W}{\sum_k W} \end{aligned}\right\} \quad \text{for } W = \Delta W - |(V_b)_k - V_{\min}|, \tag{4}$$

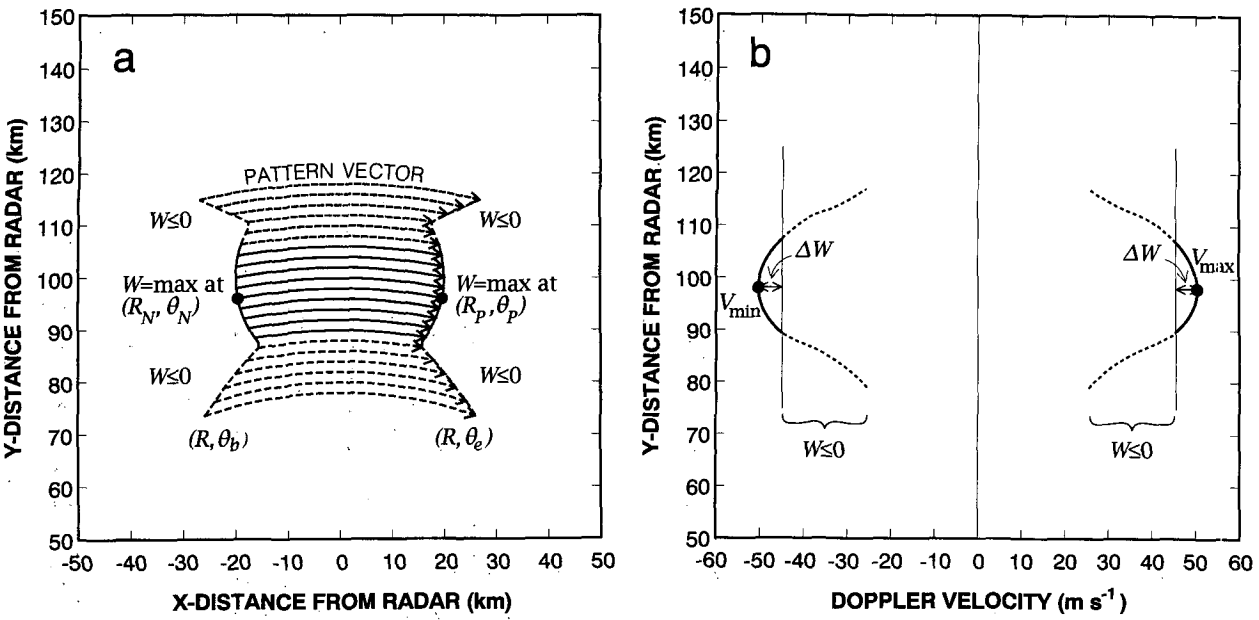

FIG. 3. (a) The pattern vector envelope defined by preset thresholds for velocity difference and azimuthal shear. Heavy dots indicate where W is maximum. (b) Profiles of the beginning and ending peak Doppler velocities along the curves shown in (a). Dashed curves are indicated for $W \leq 0$. Heavy dots indicate peak Doppler velocity values (V_{max}, V_{min}). Other parameters are defined in the text.

$$\left.\begin{aligned} V_P &= \frac{\sum_k (V_e)_k W}{\sum_k W} \\ R_P &= \frac{\sum_k (R)_k W}{\sum_k W} \\ \theta_P &= \frac{\sum_k (\theta_e)_k W}{\sum_k W} \end{aligned}\right\} \quad \text{for } W = \Delta W - |(V_e)_k - V_{max}|, \tag{5}$$

where W is confined to $0 < W \leq \Delta W$ (Fig. 3). Note that ΔW is the difference between a given velocity and the peak value shown in Fig. 3b. The values on the left-hand sides of (4) and (5) are the Doppler velocity values and velocity couplet endpoint locations, which are determined by a process that weights toward the largest velocity values. This weighting technique for tropical cyclone parameters provides estimates of rotational velocity that generally are within 3% of visually derived estimates. Note that the dashed curves shown in Fig. 3 indicate that (4) and (5) are not calculated whenever $W \leq 0$. The number of saved pattern vectors (indicated by both solid and dashed curves in Fig. 3a) must be greater than those in which W is confined to $0 < W \leq \Delta W$ (indicated by only the solid curves in this figure). The choice of ΔW depends empirically on the shape of the beginning and ending Doppler velocity profiles, which are a function of tropical cyclone size and strength. For a weak tropical cyclone circulation whose profile of tangential wind outside the RMW is nearly flat, ΔW must be as small as 3 m s^{-1}. For an intense, mature hurricane having the steep profile of tangential wind outside the RMW, $\Delta W = 5$ m s^{-1} is sufficient, as in the example of Fig. 3b. The computation of the weighted values V, R, and θ in (4) and (5) is sensitive to the choice of ΔW. The larger the ΔW value, the more the weighted values depart from their true values. Therefore, it is proposed that

$$\Delta W = 3 \text{ m s}^{-1}, \quad \text{for} \quad \Delta \bar{V} < 35 \text{ m s}^{-1}, \tag{6}$$

$$\Delta W = 5 \text{ m s}^{-1}, \quad \text{for} \quad \Delta \bar{V} \geq 35 \text{ m s}^{-1}, \tag{7}$$

where $\Delta \bar{V} = (V_{max} - V_{min})/2$ is the average of peak Doppler velocity values obtained readily from the pattern vectors.

b. *Estimation of center location*

After (4) and (5) are computed, the next step is to calculate an estimated range from the radar to Doppler velocity peaks at N and P. Following Wood and Brown (1992), the estimated range R_E is represented by

$$R_E = F\left(\frac{R_N + R_P}{2}\right), \tag{8}$$

where $(R_N + R_P)/2$ is the average of the ranges from the radar to an apparent signature center. Here, the correction factor F can be estimated from the observed angle $\Delta\theta$ using the following relation:

$$F = \sec\left(\frac{\Delta\theta}{2}\right), \quad 0° \leq |\Delta\theta| < 180°, \tag{9}$$

where $\Delta\theta = \theta_P - \theta_N$ is the observed azimuth angle difference between the two peak Doppler velocity values at N and P. Without the correction factor, the difference between the estimated range and the true range from the radar to the center position would become increasingly large as the region of maximum winds of a large, axisymmetric circulation approached the radar, as reported by Wood and Brown (1992). The estimated azimuth of the signature center (θ_E) from the radar is the average of θ_N and θ_P; that is, $\theta_E = (\theta_N + \theta_P)/2$.

4. Test of the tropical cyclone center detection technique

The technique developed in the foregoing discussion is evaluated here to determine its ability to detect a tropical cyclone center. Because the Wood and Brown (1992) technique was designed for determining the center position of a large, axisymmetric wind circulation at a short range, it is necessary to experimentally test the performance of the center-finding technique by using different ranges and viewing directions relative to real tropical cyclone wind asymmetries.

a. Simulated Doppler velocities

Doppler velocity component V_d at slant range R and elevation angle ϕ is the component of the three-dimensional wind vector in the viewing direction θ from the radar and is given by (e.g., Doviak and Zrnić 1984, p. 262)

$$V_d = u\cos\phi\sin\theta + v\cos\phi\cos\theta + (w + V_t)\sin\phi, \tag{10}$$

where u, v, and w are, respectively, the velocity components directed eastward, northward, and upward, and V_t is the terminal fall speed (negative) of precipitation particles. The range and azimuth from the radar to a storm circulation center must be defined in order to generate Doppler velocities. Equation (10) was used to produce WSR-88D-like Doppler radar data simulating the scan of a ground-based Doppler radar through a gridded volume of hurricane wind field data.

b. Hurricane Alicia

Willoughby et al. (1984) analyzed in situ aircraft observations in a moving, circular domain within 150 km of the storm center of a hurricane. The storm center position was objectively identified from the flight-level winds using the technique described by Willoughby and Chelmow (1982). Willoughby's (1985) analysis was applied to Hurricane Alicia (1983) to reconstruct the gridded wind field from aircraft measurements at the 850-mb level, which was evaluated on a two-dimensional array with a 5-km grid spacing. Because the gridded aircraft data were at an altitude of 1.5 km, it is assumed that the hurricane was far enough from the radar. Also the data were obtained at a 0° elevation angle, and therefore the last term on the right-hand side of (10) can be ignored.

A scenario is considered here in which the simulated hurricane (Alicia) approaches a coastline, in this case, the Houston–Galveston area, where a WSR-88D system is located. This scenario is presented in Fig. 4. Given the radar site and flight-level storm center position in terms of latitude and longitude, the range and azimuth from the radar to the center position can be calculated. The low-altitude structure of the Alicia wind field at 0300 UTC 17 August 1983, 1500 UTC 17 August 1983, and 0300 UTC 18 August 1983 is, respectively, shown in Figs. 4a–c. The northwest-translating storm reached hurricane intensity at 0000 UTC 17 August (Powell 1987). During the 24-h period beginning 3 h later, the radius of the inner wind maximum decreased from about 40 to 20 km, and an outer wind maximum formed at a greater radius of about 100 km from the storm center as Hurricane Alicia approached the Texas coast.

Simulated Doppler velocity patterns that correspond to the Alicia wind fields are shown in Figs. 4d–f. Because a WSR-88D produces velocity data out to a maximum of 230 km (Crum and Alberty 1993), an approaching tropical cyclone will first be seen using only reflectivity data (out to 460 km). The circulation center at 0300 UTC 17 August was beyond the 230-km range; therefore, Fig. 4d does not show a couplet of closed isodops of opposite Doppler velocities. Between 0900 UTC 17 August and 0300 UTC 18 August, peak Doppler velocity values increased in magnitude and the diameter of the couplet contracted steadily in response to the contraction of the inner concentric eye (Willoughby et al. 1984).

Velocity difference ΔV and azimuthal shear S thresholds for the detection of tropical cyclones have not yet been established because of the lack of data. However, such thresholds were arbitrarily determined for this study: 50 m s^{-1} for the velocity difference threshold and 0.5 m s^{-1} km^{-1} for the azimuthal shear detection threshold.

Table 1 summarizes the tropical cyclone center positions estimated from simulated single Doppler radar and in situ aircraft measurements between 0900 UTC 17 August 1983 and 0300 UTC 18 August 1983. The average of peak Doppler velocity values across the hurricane vortex core diameter, denoted by $\bar{V}_d = (V_P - V_N)/2$, changed with time and is also shown in the table. The fluctuation in $\bar{V}_d$ resulted from temporal changes in the asymmetric structure of the tangential wind and overall change in hurricane intensity. While Alicia intensified, tangential wind asymmetric patterns rotated from time to time, as can be seen in Figs. 4a–c. When a tangential wind maximum was in the front quadrant of Alicia (Fig. 4b), the corresponding Doppler velocity pattern (Fig. 4e), as viewed from the radar, was quasi-axisymmetric. When Alicia approached the radar with its strongest winds in the left quadrant (Fig. 4c), the Doppler velocity pattern was asymmetric (Fig.

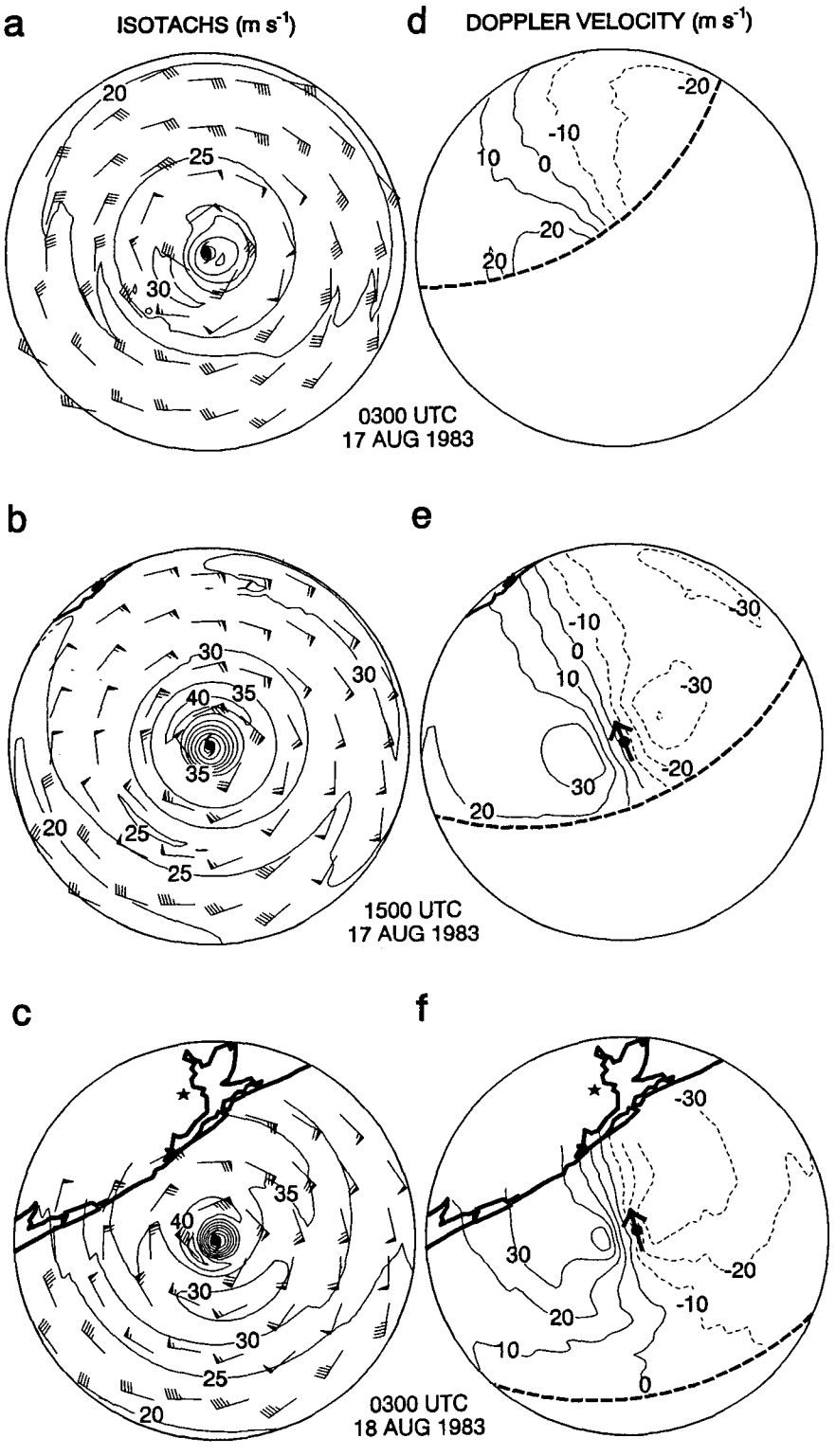

FIG. 4. (a)–(c) Analyses of the ground-relative wind speed (m s^{-1}) in Hurricane Alicia as it made landfall on the Texas coast at (a) 0300 UTC 17 August 1983, (b) 1500 UTC 17 August 1983, and (c) 0300 UTC 18 August 1983 (after Willoughby 1985). The contour interval is 5 m s^{-1}; the wind-plotting convention is the same as in Fig. 1. The hurricane center is indicated by the hurricane symbol. (d)–(e) Corresponding simulated Doppler velocity patterns of the Alicia flow field relative to the current WSR-88D radar site [indicated by a solid star in panels (c) and (f)] in the Houston–Galveston area. The Doppler velocity contour convention is the same as in Fig. 1. The heavy, dashed arc represents a 230-km range. The solid dot represents an estimated position of the signature center from the radar; the heavy arrow centered on the solid dot represents the direction to the radar. In panels (b), (c), (e), and (f) the coastline is indicated by heavy lines.

TABLE 1. Average peak Doppler velocity $\bar{V}_d$ values across the core diameter, and storm center positions estimated from simulated land-based Doppler radar measurements and in situ aircraft measurements for the Hurricane Alicia case. The elevation angle was 0°.

Time (UTC)	$\bar{V}_d$* (m s^{-1})	Storm center*	Storm center**	Storm center difference (km)
17 August 1983				
0900	34	27.968°N, 93.945°W	27.910°N, 94.000°W	8.4
1200	38	27.907°N, 94.317°W	27.910°N, 94.330°W	1.3
1500	40	27.970°N, 94.338°W	27.970°N, 94.360°W	2.1
1800	44	28.062°N, 94.339°W	28.070°N, 94.360°W	2.3
2100	41	28.382°N, 94.651°W	28.370°N, 94.660°W	1.0
18 August 1983				
0000	41	28.504°N, 94.638°W	28.480°N, 94.680°W	4.9
0300	43	28.504°N, 94.825°W	28.500°N, 94.850°W	2.5

* Determined from simulated land-based Doppler radar measurements.
** Determined from in situ aircraft measurements.

4f). The decrease of $\bar{V}_d$ between 1800 and 2100 UTC, shown in Table 1, could be mistaken for a weakening hurricane. However, from a forecasting point of view, it is important to recognize the change of closed isodops of opposite Doppler velocities on both sides of the signature center that indicate temporal rotation of the wind asymmetric pattern relative to the radar-viewing direction. Notice in Fig. 4d that an estimated signature center was not calculated, since the Alicia circulation center at 0300 UTC 17 August 1983 was beyond the 230-km range associated with the Doppler velocity mode.

Estimated ranges R_E and azimuths θ_E of the signature center of Alicia from the radar were converted into latitudes and longitudes that were compared with storm center positions determined using in situ aircraft measurements and the Willoughby and Chelmow (1982) technique. The differences between center positions estimated from simulated single Doppler radar and in situ aircraft measurements, shown in Table 1, indicate a good correlation between the estimates. At 0900 UTC 17 August 1983, the difference between the center positions is somewhat large. This is due in part to the radii of the inner wind maximum on one side of the Alicia circulation center being greater than those on the opposite side. This is a result of asymmetric convection in the inner eyewall. It may cause the cyclone center to move erratically some tens of kilometers in a few hours (Willoughby 1990). In this case, the disadvantage of using the center azimuth θ_E is obvious, since the Wood and Brown (1992) technique cannot be applied to an asymmetric hurricane circulation.

c. *Hurricane Gloria*

Airborne Doppler-derived, three-dimensional radar reflectivity and wind fields of Gloria were obtained to further test the concept of using ground-based Doppler radar data to estimate tropical cyclone center location. Three-dimensional analyses of these fields of the Gloria eye were discussed in detail by Franklin et al. (1988, 1993). The fields covered a 147 km × 147 km region centered on the storm circulation center position determined from the Willoughby and Chelmow (1982) technique. The gridded analysis was extended from 0.5 to 14 km in altitude. The horizontal and vertical resolutions of the Doppler analysis were 3 and 0.5 km, respectively.

Table 2 lists cyclone center positions with various heights. Each center position was computed from the center of vorticity maximum and represents the best center position in a moving vortex system, according to F. D. Marks Jr. of the National Oceanographic and Atmospheric Administration's (NOAA) Atlantic Oceanographic and Meteorological Laboratory/Hurricane Research Division (AOML/HRD) (1993, personal communication). Note that the vorticity center positions were just to the northeast of the flight-level mean storm center position, as indicated in Table 2. The main reason for the displacement of the vorticity centers to the right of Gloria's track was that the centers were earth relative for the purpose of navigation. Willoughby and Chelmow (1982) described the difference

TABLE 2. Storm center positions at different heights, determined from the center of maximum vorticity in a moving vortex system of Hurricane Gloria. The mean storm center position at the flight level was 24.568°N, 69.916°W at 0059 UTC 25 September 1985. Gloria was moving from 148° at 4.1 m s^{-1} (provided by staff of AOML/HRD).

Height (km)	Latitude	Longitude
0.5	24.614°N	69.884°W
1.0	24.596°N	69.884°W
1.5	24.598°N	69.888°W
2.0	24.591°N	69.883°W
2.5	24.597°N	69.889°W
3.0	24.595°N	69.891°W
3.5	24.598°N	69.890°W
4.0	24.598°N	69.890°W
4.5	24.598°N	69.890°W
5.0	24.618°N	69.889°W

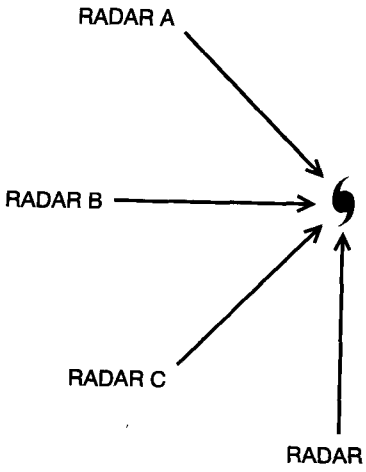

FIG. 5. Four different radar locations relative to the flight-level storm center position of Hurricane Gloria.

between the earth- and storm-relative centers and track. The storm-relative track paralleled and lay to the right of the earth-relative track. In the case of Gloria, it was about 3 km to the right in the mean overall altitudes, as shown in Table 2.

Four different ranges and azimuths from the radar to the flight-level center location were selected and are shown in Fig. 5. In this case, the velocity difference and azimuthal shear detection thresholds were chosen as 60 m s^{-1} and 1.0 m s^{-1} km^{-1}, respectively. As viewed from each radar location, ground-based Doppler radar–estimated cyclone center positions were compared with objective cyclone center position, and are shown in Table 3. The latter positions were interpolated to the radar's height location of storm center position for the purpose of comparison with radar-estimated cyclone center positions at slant range. The storm center differences shown in Table 3 indicate that the center-finding technique performed well for detecting center location estimates from the radar measurements for radars A–C compared with center positions determined from in situ aircraft measurements. As viewed from radar D, differences between these center location estimates were somewhat larger. This was because when the radius of maximum wind was perpendicular to radar D, and to the right of the storm center, it was smaller than that to the left. Again, the center azimuth θ_E can cause problems in centering because of asymmetries in the wind field.

5. Conclusions and discussions

A tropical cyclone center-finding technique for land-based Doppler radar determination of the center position in tropical cyclones approaching land has been developed and applied to the wind field data collected by reconnaissance aircraft during Hurricanes Alicia (1983) and Gloria (1985). Preliminary results show that the estimated locations of the hurricane vortex signature centers from the radar compare favorably with objective center positions determined from the Willoughby and Chelmow (1982) technique and according to Marks (1993, personal communication). Automated determination of the cyclone center position and its motion are very important for issuing timely information. Center positions identified in suc-

TABLE 3. Storm center positions estimated from simulated land-based Doppler radar measurements and in situ aircraft measurements for the Hurricane Gloria case. Different radar ranges and azimuths relative to the storm center are as shown in Fig. 5. The elevation angle was 0.5°. Height was computed from the estimated center range, which accounts for the earth's curvature.

Radar	Range (km)	Height (km)	Storm center*	Storm center**	Storm center difference (km)
A	50	0.63	24.596°N, 69.851°W	24.610°N, 69.884°W	3.6
	100	1.44	24.613°N, 69.882°W	24.598°N, 69.888°W	1.8
	150	2.61	24.605°N, 69.890°W	24.597°N, 69.889°W	0.9
	200	4.08	24.593°N, 69.896°W	24,598°N, 69.890°W	0.8
B	50	0.68	24.606°N, 69.855°W	24.608°N, 69.884°W	3.0
	100	1.55	24.592°N, 69.875°W	24.597°N, 69.888°W	1.4
	150	2.70	24.581°N, 69.892°W	24.596°N, 69.890°W	1.7
	200	4.12	24,566°N, 69.911°W	24.598°N, 69.890°W	4.2
C	50	0.68	24.619°N, 69.882°W	24.607°N, 69.884°W	1.4
	100	1.59	24.610°N, 69.873°W	24.597°N, 69.887°W	2.0
	150	2.81	24.608°N, 69.865°W	24.596°N, 69.890°W	2.9
	200	4.29	24.597°N, 69.867°W	24.598°N, 69.890°W	2.4
D	50	0.60	24.579°N, 69.933°W	24.610°N, 69.884°W	6.0
	100	1.45	24.561°N, 69.944°W	24.598°N, 69.888°W	7.0
	150	2.63	24.566°N, 69.947°W	24.596°N, 69.890°W	6.7
	200	4.14	24.579°N, 69.941°W	24.598°N, 69.890°W	5.6

* Determined from simulated land-based Doppler radar measurements.
** Determined from in situ aircraft measurements (Table 2) and interpolated for height.

ceeding radar volumetric scans are correlated in time to provide a smooth storm track that could be used to forecast future center positions. In addition to center position calculations, the Doppler technique is valuable in determining the maximum wind speed and the radius of the maximum wind speed, which are essential for storm surge calculations.

Although the performance of the tropical cyclone center-finding technique presented here is encouraging, this technique is limited by the circulation asymmetry or ellipticity of natural hurricanes, which cause problems in locating the eye center. This is a particularly troublesome error source for calculations of center location estimates, because the Wood and Brown (1992) technique on which the current technique was based was designed for determining the center position of a large, axisymmetric wind circulation. Tropical cyclone center-finding evaluations need to be performed over many WSR-88D cases before greater statistical confidence in the technique's performance can be achieved.

Future testing should include the study of eyewall radar reflectivity data, which will eliminate Doppler wind information where reflectivity values are below a threshold suitable for velocity measurements. The pattern vectors of many hurricanes may be interrupted by regions of little or no rain, where reflectivities are below detection threshold. When hurricanes are viewed from a Doppler radar, it is critical that a couplet of closed contours of opposing Doppler velocities on both sides of the eyewall reflectivity region be present for center position computation. If either side of the couplet is absent, the center position will not be calculated, thereby producing a gap in the track. The task of estimating a tropical cyclone center location is difficult in a situation where the precipitation in tropical storms and weak hurricanes is organized in rainbands that may not encircle the storm center completely. In a reasonably symmetric storm with a closed eyewall, the storm's center is easily identified and is a good approximation of the storm position.

One aspect of the center-finding technique that needs to be improved is the magnitude of the azimuthal shear and velocity difference criteria for pattern vector identification of tropical cyclone center positions. Determination of the criteria depends upon the tropical cyclone size and strength. In different hurricanes, maximum horizontal winds occur 10–50 km from the storm center and 0.5–1 km above the ocean surface (Burpee 1986). An observer may subjectively determine the azimuthal shear and velocity difference thresholds by obtaining low-altitude wind maximum and eye diameter estimates from hurricane reconnaissance flights or from ships and buoys that provide occasional observations of low-altitude winds. Another point to bear in mind is that the criteria need to be different from those defined in a mesocyclone detection algorithm. This is important, because a hurricane mesocyclone that appeared in analyses of airborne Doppler radar measurements done by Marks and Houze (1984) in the eyewall of Hurricane Debby (1982) occurred well out over the ocean. The tropical cyclone center-finding technique could inadvertently detect the center position of mesocyclones or highly localized shear zones if the azimuthal shear and/or velocity difference criteria were improperly defined. The upper limit of the shear and velocity difference thresholds for a mesocyclone detection algorithm have not yet been defined and could be considered in the near future.

Marks (1990) pointed out that there were discrepancies between WSR-57 reflectivity centers and wind-derived centers estimated from airborne Doppler observations of tropical cyclones. On the basis of a study of Hurricane Frederic (1979), Marks found that the hurricane reflectivity-based center determined from the National Weather Service's WSR-57 radar in Slidell, Louisiana, was different from an airborne Doppler-derived wind center. The reflectivity-derived center was determined from the centroid of the oval reflectivity maximum, whereas the wind center was observed closer to the more intense portion of the eyewall reflectivity maximum as a result of asymmetric convection. In some tropical cyclones, the position of the wind center with respect to the reflectivity center rotated around inside the eye, often in response to changes in the position of the intense reflectivity in the eyewall, and thus caused a trochoidal oscillation in the storm track (e.g., Lewis and Black 1977). As suggested by Marks (1990), a combination of noncoherent and coherent radar observations may be necessary to determine storm position.

Both Doppler velocity- and reflectivity-based techniques are needed to identify and track tropical cyclone centers using the coastal WSR-88D radars because of the range limitations for the Doppler data. Eye center estimates based on reflectivity patterns of the spiral rainbands and eyewalls are obtained at distances between 230 and 460 km from the radar, where Doppler velocities are not available. At distances less than 230 km, where Doppler velocities are estimated, a determination of the location of the center is obtained from a velocity-based technique. When the tropical cyclone center is within 230 km, the center-finding techniques based on *both* Doppler velocity and reflectivity information are needed not only to provide center location estimates to forecasters but also to supply such important information as a trochoidal oscillation in the storm track and the relative orientation of the reflectivity- and wind-derived centers. In the future, considerable applications research will include the analyses of comparisons between reflectivity-derived centers and Doppler velocity-derived centers. It would be useful to understand how the Doppler technique compares with reflectivity-based techniques.

Acknowledgments. The author appreciates the reviews of Dave Jorgensen, Rodger Brown, Mike Eilts, and Arthur Witt of the NOAA/Environmental Research Laboratory (ERL) National Severe Storms

Laboratory, and Ralph Donaldson of Hughes STX Corporation, who provided valued comments on the manuscript. Review by and discussions with Wen-Chau Lee of the National Center for Atmospheric Research were especially helpful. The author appreciates the thorough reviews of and helpful suggestions from two anonymous reviewers. The author is very grateful to Frank Marks and Hugh Willoughby of the NOAA/ERL/AOML Hurricane Research Division for supplying the gridded Gloria and Alicia wind data, respectively. Joan Kimpel assisted with figure preparation.

REFERENCES

Baynton, H. W., 1979: The case for Doppler radars along our hurricane affected coasts. *Bull. Amer. Meteor. Soc.*, **60,** 1014–1023.

Brown, R. A., and V. T. Wood, 1983: Improved severe storm warnings using Doppler radar. *Natl. Wea. Dig.*, **8,** 17–27; errata, **9,** 2.

——, and ——, 1991: On the interpretation of single-Doppler velocity patterns within severe thunderstorms. *Wea. Forecasting,* **6,** 32–48.

Burgess, D. W., and P. S. Ray, 1986: Principles of radar. *Mesoscale Meteorology and Forecasting,* P. S. Ray, Ed., Amer. Meteor. Soc., 85–117.

——, and L. R. Lemon, 1990: Severe thunderstorm detection by radar. *Radar in Meteorology,* D. Atlas, Ed., Amer. Meteor. Soc., 619–647.

Burpee, R. W., 1986: Mesoscale structure of hurricanes. *Mesoscale Meteorology and Forecasting,* P. S. Ray, Ed., Amer. Meteor. Soc., 311–330.

Crum, T. D., and R. L. Alberty, 1993: The WSR-88D and the WSR-88D operational support facility. *Bull. Amer. Meteor. Soc.,* **74,** 1669–1687.

Desrochers, P. R., and R. J. Donaldson Jr., 1992: Automatic tornado prediction with an improved mesocyclone detection algorithm. *Wea. Forecasting,* **7,** 373–388.

Donaldson, R. J., Jr., 1991: A proposed technique for diagnosis by radar of hurricane structure. *J. Appl. Meteor.*, **30,** 1636–1645.

Doviak, R. J., and D. S. Zrnić, 1984: *Doppler Radar and Weather Observations.* Academic Press, 458 pp.

Franklin, J. L., S. J. Lord, and F. D. Marks, Jr., 1988: Dropwindsonde and radar observations of the eye of Hurricane Gloria (1985). *Mon. Wea. Rev.*, **116,** 1237–1244.

——, ——, S. E. Feuer, and F. D. Marks Jr., 1993: The kinematic structure of Hurricane Gloria (1985) determined from nested analyses of dropwindsonde and Doppler radar data. *Mon. Wea. Rev.*, **121,** 2433–2451.

Gray, W. M., and D. J. Shea, 1973: The hurricane's inner core region. II: Thermal stability and dynamic characteristics. *J. Meteor.,* **30,** 1565–1576.

Hughes, L. A., 1952: On the low level wind structure of tropical cyclones. *J. Meteor.*, **9,** 422–428.

Jorgensen, D. P., 1982: The organization and structure of hurricane convective bands with application to NEXRAD. *Proc. NEXRAD Doppler Radar Symp./Workshop,* P. S. Ray and K. Colbert, Eds., Norman, OK, Cooperative Institute for Mesoscale Meteorological Studies, University of Oklahoma, 67–81.

Lee, W.-C., B. J.-D. Jou, and B.-L. Chang, 1993: Nowcasting typhoon circulation using Doppler radar: The ground-based VTD (GBVTD) technique. Preprints, *26th Int. Conf. on Radar Meteorology,* Norman, OK, Amer. Meteor. Soc., 83–87.

Lewis, B. M., and P. G. Black, 1977: Spectral analysis of oscillations of radar-determined hurricane tracks. Preprints, *11th Technical Conf. on Hurricanes and Tropical Meteorology,* Miami Beach, FL, Amer. Meteor. Soc., 484–489.

Marks, F. D., Jr., 1990: Radar observations of tropical weather systems. *Radar In Meteorology,* D. Atlas, Ed., Amer. Meteor. Soc., 401–425.

——, and R. A. Houze Jr., 1984: Airborne Doppler radar observations in Hurricane Debby. *Bull. Amer. Meteor. Soc.*, **65,** 569–582.

Maynard, R. H., 1945: Radar and weather. *J. Meteor.*, **2,** 214–226.

Powell, M. D., 1987: Changes in the low-level kinematic and thermodynamic structure of Hurricane Alicia (1983) at landfall. *Mon. Wea. Rev.*, **115,** 75–99.

Rankine, W. J. M., 1901: Motions of fluids. *A Manual of Applied Mechanics,* 16th ed., Charles Griff and Company, 574–578.

Riehl, H., 1954: *Tropical Meteorology.* McGraw-Hill, 392 pp.

——, 1963: Some relations between wind and thermal structure of steady-state hurricanes. *J. Atmos. Sci.*, **20,** 276–287.

Roux, F., 1993: Real-time analysis of Doppler data in tropical cyclones: Application of "EVTD" to airborne dual-beam and ground-based radars. Preprints, *20th Conf. on Hurricanes and Tropical Meteorology,* San Antonio, TX, Amer. Meteor. Soc., 439–442.

Senn, H. V., and H. W. Hiser, 1959: On the origin of hurricane spiral bands. *J. Meteor.*, **16,** 419–426.

——, ——, and R. C. Bourret, 1957: Studies of hurricane spiral bands as observed on radar. Final Report, U.S. Weather Bureau Contract No. Cwb-9066, University of Miami, 21 pp. [NTIS-PB-168367.]

Sivaramakrishnan, M. V., and M. Selvam, 1966: On the use of the spiral-overlay technique for estimating the center positions of tropical cyclones from satellite photographs taken over the Indian region. *Proc. 12th Conf. on Radar Meteorology,* Norman, OK, Amer. Meteor. Soc., 440–446.

Wexler, H., 1947: Structure of hurricanes as determined by radar. *Ann. N.Y. Acad. Sci.*, **48,** 821–844.

Willoughby, H. E., 1985: Confirmatory observations of concentric eyes in hurricanes. *Extended Abstracts, 16th Conf. on Hurricanes and Tropical Meteorology,* Houston, TX, Amer. Meteor. Soc., 1–2.

——, 1990: Temporal changes of the primary circulation in tropical cyclones. *J. Atmos. Sci.*, **47,** 242–264.

——, and M. B. Chelmow, 1982: Objective determination of hurricane tracks from aircraft observations. *Mon. Wea. Rev.*, **110,** 1298–1305.

——, F. D. Marks Jr., and R. F. Feinberg, 1984: Stationary and moving convective bands in hurricanes. *J. Atmos. Sci.*, **41,** 3189–3211.

Wood, V. T., and R. A. Brown, 1992: Effects of radar proximity on single-Doppler velocity signatures of axisymmetric rotation and divergence. *Mon. Wea. Rev.*, **120,** 2798–2807.

Zipser, E., A. Betts, F. Ruggiero, and B. Hinton, 1990: Tropical meteorology: Panel report. *Radar In Meteorology,* D. Atlas, Ed., Amer. Meteor. Soc., 426–432.

Zrnić, D. S., D. W. Burgess, and L. D. Hennington, 1985: Automatic detection of mesocyclonic shear with Doppler radar. *J. Atmos. Oceanic Technol.*, **2,** 425–438.